Physics of the Earth and Planetary Interiors 181 (2010) 73–81

Contents lists available at ScienceDirect

Physics of the Earth and Planetary Interiors

journal homepage: www.elsevier.com/locate/pepi

S-wave attenuation characteristics in the Galeras volcanic complex (south western Colombia)

Arantza Ugalde[a,*], Eduard Carcolé[b], Carlos A. Vargas[c,1]

[a] Observatori de l'Ebre, CSIC – Universitat Ramon Llull, Horta Alta, 38, 43520 Roquetes (Tarragona), Spain
[b] Department of Geophysics, Graduate School of Science, Tohoku University, Aramaki-Aza-Aoba 6-3, Aoba-ku, Sendai-shi, Miyagi-ken 980-8578, Japan
[c] Departamento de Geociencias, Universidad Nacional de Colombia, Bogotá, Colombia

ARTICLE INFO

Article history:
Received 22 April 2008
Received in revised form 13 April 2010
Accepted 29 April 2010

Edited by: G. Helffrich.

Keywords:
Coda waves
Scattering
Intrinsic absorption
Galeras volcano

ABSTRACT

Vertical-component, short period seismograms from 435 well located volcano-tectonic earthquakes are used to estimate S-wave attenuation in the Galeras volcanic complex (south western Colombia) using coda waves. The coda magnitudes (M_c) of the events are less than 2. Event depths are less than 10 km and hypocentral distances up to 16 km. Intrinsic absorption (Q_i^{-1}) and scattering attenuation (Q_s^{-1}) are estimated by means of a fitting procedure between the observed and synthetic coda envelopes in four frequency bands (1–2, 2–4, 4–8, and 8–12 Hz). The observations are compared with the theoretical predictions by an accurate approximate analytical solution of the radiative transfer equation which is based on the assumptions of multiple isotropic scattering, impulsive isotropic point source, and a medium with homogeneous scattering and absorption properties. Results show that scattering is strong and it constitutes the predominant attenuation effect in this region. In the frequency range analyzed in this study the values of the mean free path for scattering of S waves range between $2.7 \leq l \leq 8.1$ km, which are clearly higher than those obtained in other volcanic regions of the world, but about two orders of magnitude smaller than average estimates for the Earth's crust. The characteristic length scale of intrinsic absorption gives values of $2.5 \leq l_a \leq 77$ km, which are on the same order as the usual values for the Earth's crust.

1. Introduction

Total seismic wave attenuation in the Earth is caused by two major mechanisms: scattering due to the interaction of seismic waves with the heterogeneities of the medium (when they are on a length scale close to the seismic wavelength) and intrinsic absorption due to anelasticity. The inverse quality factors, Q_i^{-1} and Q_s^{-1} characterize intrinsic absorption, and scattering attenuation, respectively, so total attenuation is the sum of the two types: $Q_t^{-1} = Q_i^{-1} + Q_s^{-1}$.

Many studies have been conducted to determine which process, intrinsic absorption or scattering, dominates total attenuation (see Sato and Fehler, 1998). Multiple scattering models for S-coda envelope synthesis have been used to separate the contribution of intrinsic absorption and scattering to total attenuation of S waves. Hoshiba (1991) estimated higher-order solutions of the multiple isotropic scattering model using numerical techniques. However, it is possible to obtain and use analytical solutions (Zeng et al., 1991; Sato, 1993). Hoshiba et al. (1991) and Fehler et al. (1992) developed the Multiple Lapse Time Window Analysis (MLTWA) to separately estimate the intrinsic absorption and scattering loss, within the framework of a model of multiple isotropic scattering in a medium with uniform distribution of scattering and absorption properties, S-wave-only scattering, constant S-wave velocity and spherically symmetrical radiation from an impulsive point source. In their method, the integrated energy density over three consecutive time windows from the S-wave arrival time is evaluated as a function of the source-receiver distance (Hoshiba, 1993). Therefore, the observed energy density is compared with the energy predicted by theoretical models to obtain the estimated scattering (g) and absorption (h) coefficients. The total attenuation, scattering loss and intrinsic absorption parameters are related to these coefficients by the expressions: $Q_t^{-1} = (g+h)v/\omega$; $Q_s^{-1} = gv/\omega$; and $Q_i^{-1} = hv/\omega$, where ω and v are the angular frequency and S-wave velocity, respectively. The MLTWA has been successfully applied to separate the contribution of scattering and intrinsic absorption from total attenuation under the hypothesis of multiple isotropic scattering in many regions of the Earth (see Ugalde et al. (2007, Figure 10) for a comparison of Q_t^{-1}, Q_i^{-1}, and Q_s^{-1} versus frequency for different regions in the world). Recently, high resolution maps of Japan for the seismic S-wave attenua-

* Corresponding author. Tel.: +34 977 500511; fax: +34 977 504660.
E-mail addresses: augalde@obsebre.es (A. Ugalde), eduard@zisin.geophys.tohoku.ac.jp (E. Carcolé), cavargasj@unal.edu.co (C.A. Vargas).
[1] Tel.: +57 1 3165000; fax: +57 1 3165390.

0031-9201/$ – see front matter © 2010 Elsevier B.V. All rights reserved.
doi:10.1016/j.pepi.2010.04.009

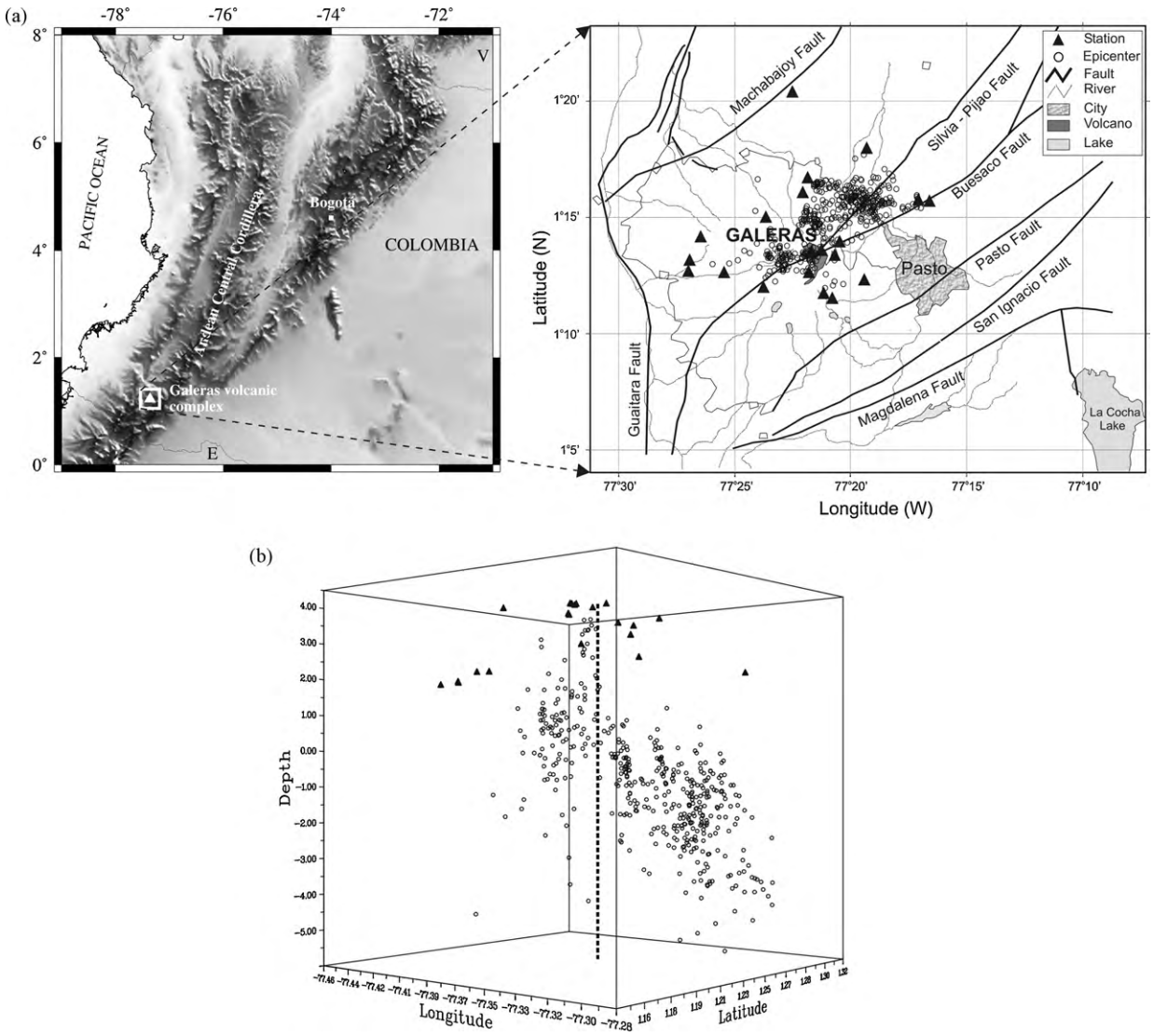

Fig. 1. (a) Topographic map of Colombia showing the location of the Galeras volcanic complex. The Central Cordillera runs along the SW–NE axis. The main faults in the region as well as the epicenters and seismic stations used are plotted; and (b) a 3-D representation of the stations and hypocenters location.

tion parameters have been obtained by using the MLTWA with data provided by the Hi-net seismic network (Carcolé and Sato, 2010). Results show strong regional variation of the parameters that depend mainly on the tectonic setting of each region and volcanism mechanisms. Although the MLTWA is based on very simple hypotheses (multiple isotropic scattering in a medium with homogeneous distribution of scattering mean free path and intrinsic absorption) the results are very informative on the characteristics of each region, and show the usefulness of studying the properties of scattered seismic waves in the understanding of the properties of the crust.

The computation of the energy density from theoretical models based on multiple isotropic scattering involves the evaluation of time-consuming two-dimensional integrals (Zeng et al., 1991) or Monte Carlo simulations (Hoshiba, 1991), which are still more time-consuming. There are two approximate solutions of the radiative transfer equation in the literature for the computation of the scattered seismic wave energy density for multiple isotropic scattering (Zeng, 1991; Paasschens, 1997). The Paasschens' (1997) expression, which is shown to be accurate and numerically very convenient, has been applied to seismological data by Abubakirov (2005) and Sens-Schönfelder and Wegler (2006).

In this study, we will focus on the estimation of S-wave attenuation in the Galeras volcanic complex (south western Colombia). Galeras was designated a Decade Volcano in 1991, which identified it as a target for intensive and interdisciplinary study during the United Nations' International Decade for Natural Disaster Reduction. Interdisciplinary research (geological, geophysical and geochemical) has been conducted in the region since the re-activation of Galeras volcano. However, to the best of our knowledge, no systematic investigation of S-wave attenuation characteristics has been performed in this region. Moncayo et al. (2004) analyzed the temporal variation of the phenomenological parameter coda-Q (Q_c) using a single-scattering model in the Galeras volcano region. Carcolé et al. (2006) imaged the small-scale heterogeneities in the same region by estimating the three-dimensional spatial distribution of relative scattering coefficients by means of a S-coda envelope inversion method. The purpose of the present study is to estimate the scattering and absorption coefficients in the Galeras volcano region. This additional contribution to the knowledge of the internal structure and properties of the Galeras volcano is of considerable practical interest because the attenuation parameters of seismic waves in the lithosphere are valuable for seismic hazard assessment in

Table 1
Layered velocity structure model considered (Diego Gómez, Vulcanological and Seismological Pasto Observatory, pers. comm.).

Depth (km)	S-wave velocity (km/s)
4	2.0
2	2.1
0	2.2
−4	3.4
−22	3.8
−40	4.5

the region. For this purpose, we will use an alternative method to analyze the contribution of intrinsic absorption and scattering to total attenuation by means of a coda envelope-fitting method using the Paasschens' (1997) solution. This method is particularly useful when the characteristics of the seismic data available do not allow using the MLTWA, as discussed in Section 4.

Other alternative methods to the MLTWA have been proposed to estimate intrinsic and scattering attenuation. In particular, Sens-Schönfelder and Wegler (2006) used a joint inversion of S-coda envelopes for source and site parameters, as well as for medium parameters assuming the theoretical model of Paasschens (1997). Matsunami and Nakamura (2004) and Del Pezzo et al. (2006) used a method based on a fitting process of the theoretical S-coda model by Zeng (1991) to an average S-coda envelope. Some other methods have been used to analyze volcanic areas (e.g., Wegler and Lühr, 2001; Wegler, 2003, 2004). Their results will be compared and discussed in Section 5.

2. Geotectonic setting and data

The Galeras volcanic complex, which is located in the Central Cordillera of the south western Colombian Andes (Fig. 1), has been intermittently active for >1 Ma. The eastern summit, called Galeras volcano (1.23°N, 77.36°W; summit elevation 4276 m), is a 4500 years old andesitic stratovolcano that is historically the most active volcano in Colombia. The tectonics of the region result from a complex interaction between the Nazca plate to the west and the South America plate to the east, which causes the uplift of the Andes and the volcanism in the region. The main tectonic feature is the Romeral fault zone, which at the same time, constitutes one of the

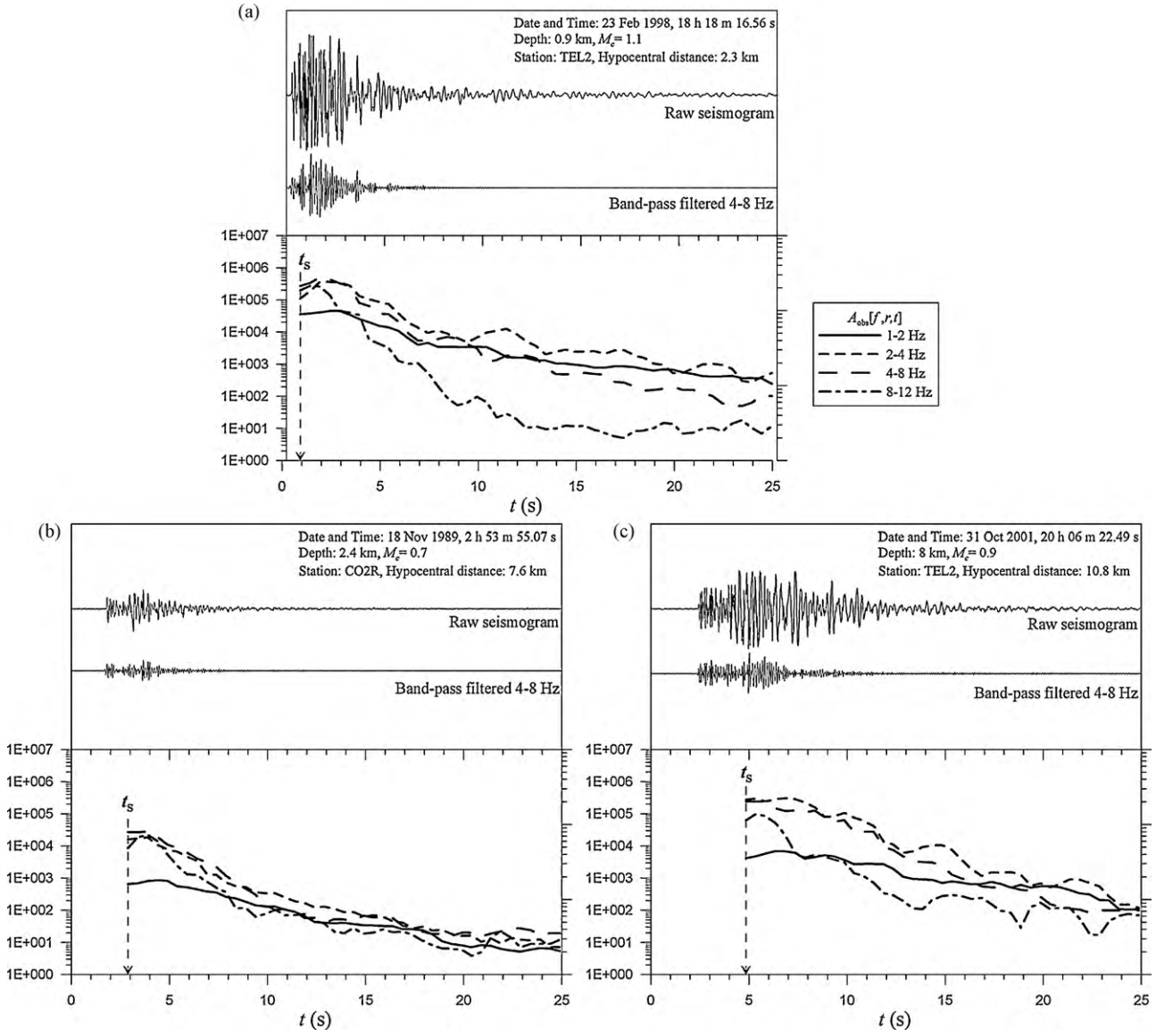

Fig. 2. Examples of the velocity recording (top) and rms amplitudes (bottom) for actual bandpass-filtered seismograms at (a) short hypocentral distance; (b) average hypocentral distance; and (c) large hypocentral distance. The depths are given with respect to a 4200 m above the sea reference level.

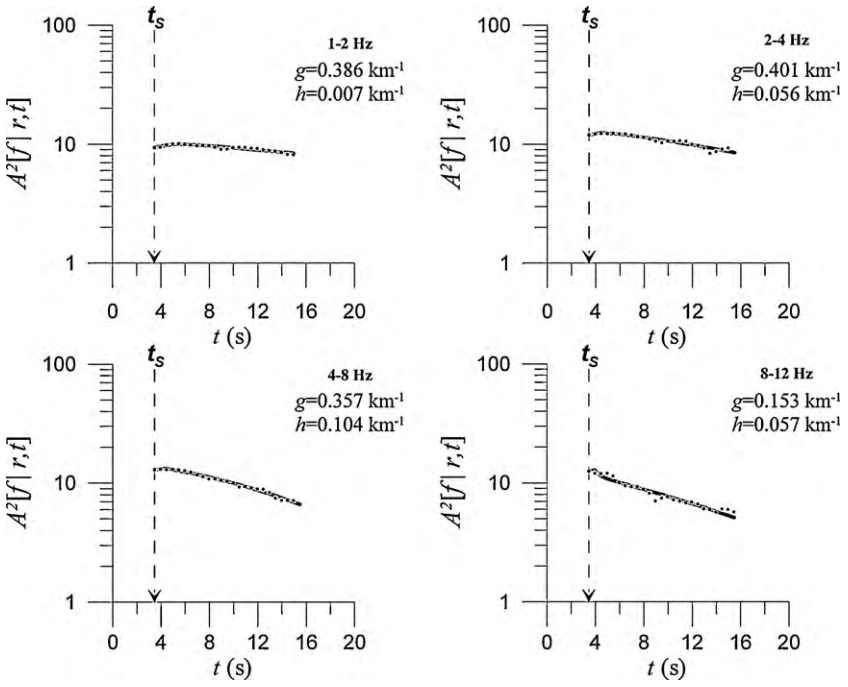

Fig. 3. (Left) Example of the bandpass-filtered mean squared amplitudes (small dots) with the prediction for best-fitting g and h parameters using Eq. (1) (solid line) for an earthquake with hypocentral distance r = 7.4 km.

main structural elements in Colombia. It includes the Silvia-Pijao and Buesaco faults that cross under the volcano structure with a N40°E trend (Fig. 1). The evolution history of the complex includes two caldera-forming eruptions (560 ka and 40 ka ago, respectively), a summit collapse, which occurred between 12 ka and 5 ka, and the present-day small cone-building style of eruption (Calvache et al., 1997).

Galeras volcano has been re-activated frequently in historic times and, although it has a short-term history (<5000 years) of relatively small-to-moderate scale eruptions, the volcanic complex has been able to produce major and hazardous eruptions. Lava flows account for more than 95% of the volcano's activity for more than 1 Ma, but modest in size explosive eruptions have also occurred during the past 10 ka and have produced pyroclastic flows frequently (Banks et al., 1997). Galeras rises 1600 m above the city of San Juan de Pasto, the capital of the State of Nariño, which is located only 9 km east from the active crater. Thus, the volcano poses potential risk to a population of more than 300,000 in Pasto and to another 100,000 people living in the flanks of the complex.

One of the four longest repose periods accounted by historical records lasted from 1948 to 1988. Then, the re-activation of Galeras volcano was recognized (Williams et al., 1990) and the eruptive period continued until 1995. This period included at least 6 explosive eruptions recorded mainly between 1992 and 1993. Since then, the volcano stayed in a relative calm stage with some ash and gas emission episodes and low-level eruptive activity (a crater located to the east of the main one was re-activated in 2002 after more than 10 years of inactivity). A new, vigorous, eruptive episode began in 2004 and 4 explosive events have been recorded up to date. Galeras volcano continues to be active at the time of this writing (April, 2008; activity reports are available at http://www.ingeominas.gov.co/ and http://www.volcano.si.edu/).

Seismicity in the region since 1988 has been characterized by long-period events, volcano-tectonic earthquakes and tremor episodes. A type of unusual shallow-source, low-frequency seismic signals called "tornillos" (screws), which are related to magmatic activity, have also been recorded during different stages of volcanic activity at Galeras (Gómez and Torres, 1997). The level of seismic activity has fluctuated between periods of low-level activity and episodes of increased earthquake rate and/or magnitude. Some shallow (up to 8 km) volcano-tectonic earthquakes have reached local magnitudes up to 4.7.

Data used in this study consist of records from 435 volcano-tectonic earthquakes over the period from 1989 through 2002 (Fig. 1). The earthquakes selected have the following mean location parameters and associated standard deviations: travel time residuals (rms) = 0.08 ± 0.02 s; azimuthal gap = 142 ± 28; horizontal error = 0.3 ± 0.1 km; and error in depth = 0.4 ± 0.2 km. Coda magnitudes are less than 2, with depths less than 6 km below the sea level, and hypocentral distances up to 16 km. The layered velocity structure adopted by the Volcanological and Seismological Pasto Observatory (Table 1) was used for the locations, which were carried out by Moncayo et al. (2004). The short-period (T_0 = 1 s), vertical component recording stations used (31 locations in total) did not operate continuously through time because of various modifications in the network configuration. The combination of telemetric and portable stations used were located at distances less than 10 km from the active crater. The recorded ground motions were digitized at a rate of 100 samples per second; the whole system has a flat velocity response between 1 and 25 Hz.

3. Theoretical background

Multiple isotropic scattering processes may be modeled by using the radiative transfer theory for the energy density (Ishimaru, 1978). The radiative transfer (or Boltzmann) equation (RTE) can be solved exactly in the Fourier space for one, two, three and four dimensions. Zeng et al. (1991) obtained an exact compact integral solution for the real three-dimensional space. In order to simplify the computations, it is possible to develop approximations of the exact solution of the RTE in three dimensions. Paasschens (1997) proposed an algebraic expression which uses the interpolation between exact solutions of the RTE for the 2-D and 4-D cases. It was successfully used by Abubakirov (2005) in a MLTWA for the Kamchatka lithosphere. Sens-Schönfelder and Wegler (2006) also

used the Paasschens' (1997) formulation to obtain source spectra and seismic moments. The solution has the form:

$$P(r,t) \simeq \frac{1}{4\pi r^2}\delta(r-vt)\exp(-vt/l)\exp(-vt/l_a) + \frac{(1-r^2/v^2t^2)^{1/8}}{(4\pi l vt/3)^{3/2}}\exp(-vt/l)\ \exp(-vt/l_a)G \times \left(\frac{vt}{l}\left[1-\frac{r^2}{v^2t^2}\right]^{3/4}\right)\Theta(vt-r) \quad (1)$$

$$G(x) = 8(3x)^{-3/2}\sum_{N=1}^{\infty}\frac{\Gamma((3/4N)+(3/2))}{\Gamma(3/4N)}\frac{x^N}{N!}$$

where v is the wave velocity, l is the mean free path for scattering, l_a is the absorption length which are related to the scattering, g, and absorption, h, coefficients by $g = 1/l$ and $h = 1/l_a$. $\Theta(x)$ is the step function, which is zero for $x < 0$ and 1 for $x > 0$. It is possible to approximate $G(x)$ within a few percent of error as $G(x) \simeq \exp(x)\sqrt{1+2.026/x}$. In Eq. (1), $P(r, t)$ represents the intensity of wave radiation spreading from the source through the medium, at distance r and time t.

There are several advantages in using an algebraic expression for synthesizing the multiple scattered wave envelopes. A very important one is the computation time, which is considerably less than for the two-dimensional integration process involved in the numerical calculation of the exact solution of the RTE. On the other hand, Eq. (1) is a very convenient expression that allows developing alternative methods to the MLTWA that can be used in any region of the world.

4. The envelope-fitting method and data analysis

The simplicity of the computation of the multiple scattered wave envelopes by means of Eq. (1) allows using alternative methodologies to the MLTWA for estimating empirically the intrinsic absorption and scattering contributions to total attenuation. In this paper we propose fitting every observed envelope by the synthetic model of Paasschens (1997) (Eq. (1)). For this purpose, we will compute the observed mean-squared (MS) seismogram envelopes ($A^2_{obs}(f, r, t)$) against lapse time for all the available narrow bandpass-filtered waveforms with center frequency f and then, a nonlinear fitting procedure will be performed between the observed and the smoothed synthetic envelopes ($A^2_{syn}(f, r, t)$), which are calculated using Eq. (1) as a function of h (=$1/l_a$) and g (=$1/l$).

Prior to this analysis, a data selection process was performed in order to discard those seismograms with saturated S-wave arrivals or poor signal-to-noise ratios. Then, each seismogram was bandpass-filtered over the frequency bands 1–2 (1.5 ± 0.5) Hz, 2–4 (3 ± 1) Hz, 4–8 (6 ± 2) Hz, and 8–12 (10 ± 2) Hz, using eight-pole Butterworth filters. The upper frequency limit is determined by the signal energy contents of the available data, which decays abruptly for frequencies f above 12 Hz. The rms amplitudes $A_{obs}(f, r, t)$ were calculated from the bandpass-filtered data by using a time window length for the averaging of $t \pm 2$ s for the frequency band centered at 1.5 Hz; $t \pm 1$ s for the 3 and 6 Hz center frequencies; and $t \pm 0.5$ for the 10 Hz center frequency. All the time windows were spaced 0.5 s. Only data with a signal-to-noise ratio greater than 2 were considered. Noise was estimated from 5 s of data preceding the P onset. Typical examples of a function $A_{obs}(f, r, t)$ for three actual seismograms used are shown in Fig. 2. All the data used in this work show clear impulsive onsets for P and S waves and a short coda. For this study, aimed to retrieve S-wave attenuation features, only vertical component data were available. Although it has been shown that the coda analysis is independent of the component of the particle ground motion (e.g., Hoshiba, 1993), the lack of horizontal component recordings to measure the direct S-wave energy may affect the final results.

The envelope-fitting method is particularly useful for the present application, because the short distance range (from 1 to 16 km) and the short duration of the S-wave coda preclude the use of the MLTWA. Depending on the frequency of interest, from 72% to 95% of the data with acceptable signal-to-noise ratios have lapse time windows of less than 25 s in length. However, in principle, the observed envelopes can be fitted to the synthetic ones which are calculated using Eq. (1) for any hypocentral distance or lapse time window. Therefore, to find the best fit model parameters g and h we performed a grid search between the observed ($A^2_{obs}(f, r, t)$) and synthetic ($A^2_{syn}(f, r, t)$) envelopes against lapse time for all the available seismograms. Before the nonlinear fitting process was performed, we smoothed the synthetic envelopes by using the same time window lengths for the averaging as for the observed data. This step is very important because the smoothing process alters the shape of the envelopes. Note that if the smoothing is not performed in the synthetic envelope, it is impossible to fit it to experimental data due to the presence of a delta function in Eq. (1).

We devised a convenient best-fitting scheme on a logarithmic scale for the ith seismogram that involves the minimization of the misfit function:

$$\chi_i^2 = \frac{1}{N}\sum_{j=1}^{N}\left[\ln(A^2_{obs}(f, r_i, t_j)) - \ln(A^2_{syn}(f, r_i, t_j)) - c_i\right]^2 \quad (2)$$

where $c_i = (1/N)\sum_{j=1}^{N}\ln[A^2_{obs}(f, r_i, t_j)] - \ln[A^2_{syn}(f, r_i, t_j)]$ accounts for the site and source effects and it is considered constant for a single frequency. N is the number of points of the time window considered. We stress in this point that in this method it is not necessary to choose an arbitrary reference time in order to carry out a normalization of the waveforms. Notice that the normalization process, which is needed in the other methods such as the MLTWA, may be sensitive to coda fluctuations and may introduce some errors in the computation of both g and h.

To automate the process, and inspired in the procedure used by Wegler and Lühr (2001), we considered the start time (t_1) of the window used for the nonlinear fit as marked by the S-wave travel time, t_S, reading on each seismogram, as information on the direct S-wave energy is required to separate intrinsic and scattering attenuation The end of the time window (t_N) corresponds to $t_S + 12$ s. This value was chosen by reaching an agreement between having the longest time window length for the fit above the noise level and rejecting the minimum data files as possible. Information on the direct S-wave energy is required to separate intrinsic and scattering attenuation. In fact, the MLTWA analyzes data starting from t_S. On the other hand, we compared the results obtained for several time window lengths (from 10 to 15 s from t_S) and they were inside the error bounds, which assures the stability of the method. The coda envelope decay after $2t_S$ (which corresponds to a lapse time of 14 s for the most distant event) shows a linear behavior for all the events.

A total of 3×10^6 pairs (g, h), $g = n \times 0.001$ ($n = 1, 2, 3, \ldots, 3000$); $h = m \times 0.001$ ($m = 1, 2, 3, \ldots, 1000$) for the synthetic energy were searched for the best fit. It is mandatory to calculate a theoretical velocity for each seismogram using the equation $v = r/t_S$ in order to use the envelope-fitting method. In this study, the S-wave velocity distribution was computed for each waveform using $v = r/t_S$ (see also Wegler and Lühr, 2001) which gives a mean value of $v = 2.23$ km/s with a standard deviation $\sigma = 0.27$. The assumption of a half space is certainly a limitation of the proposed methodology, since estimates of g and h may depend on the velocity structure of the region, as pointed out by Hoshiba et al. (2001).

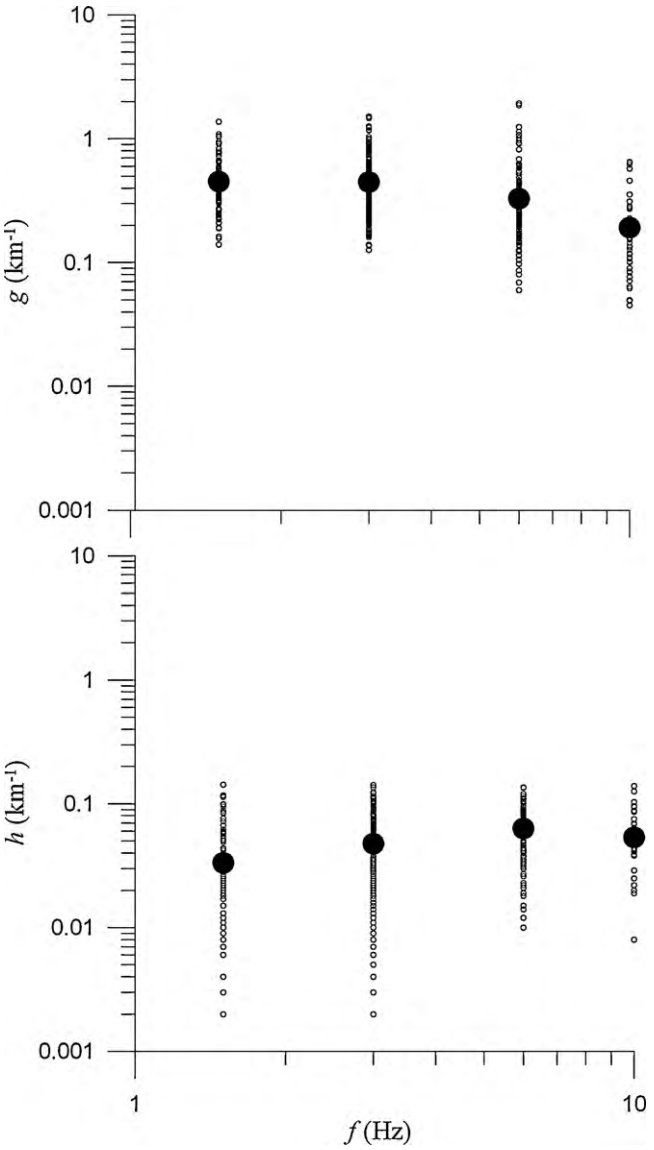

Fig. 4. Estimates of g (top) and h (bottom) as a function of frequency. A dot indicates a single estimate for each hypocenter-station path and the largest circles represent the mean value.

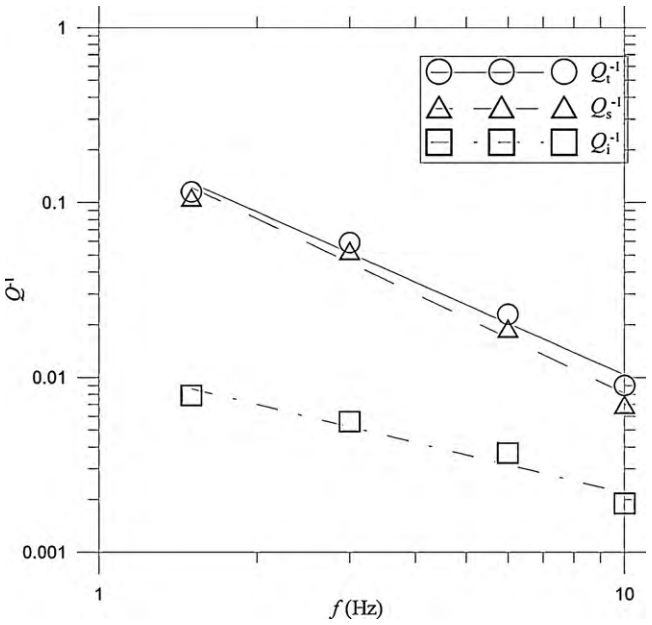

Fig. 5. Comparative plot of Q_i^{-1}, Q_s^{-1}, and Q_t^{-1} as a function of frequency.

Final values for g and h for the study region are obtained by averaging the single estimates from every envelope for each analyzed frequency band.

5. Results and discussion

5.1. Attenuation parameters

Fig. 3 shows an example of the best-fitting theoretical envelopes along with the observed ones against time for each frequency band studied. In this example the g and h estimates are within one standard deviation of the mean g and h values for all the analyzed frequency bands. All the estimated values and averages are plotted in Fig. 4, where each small circle represents g and h from a single seismogram. We note that, after the visual inspection of the whole seismograms collection, that corresponded to 435 earthquakes recorded at 31 stations during 14 years (September, 1988 to June, 2002), we got 1953 seismograms, and after the strict quality control procedures considered in the computing processes, we only got final results for 110 seismograms at 1.5 Hz, 399 seismograms at 3 Hz, 183 seismograms at 6 Hz, and 50 seismograms at 10 Hz center frequencies. The mean attenuation parameters ($\bar{g}$, $\bar{h}$, and their inverses $\bar{l}$ and $\bar{l}_a$) for the study region were obtained by averaging the g, h, l and l_a estimates computed for every single hypocenter-station path. They are shown in Table 2, together with the corresponding Q_i^{-1} (intrinsic absorption), Q_s^{-1} (scattering attenuation) and Q_t^{-1} (total attenuation) mean values, which were calculated from $\bar{g}$ and $\bar{h}$ by considering an average S-wave velocity value of $\bar{v} = 2.23$ km/s. Fitting $\bar{Q}_i^{-1}$, $\bar{Q}_s^{-1}$ and $\bar{Q}_t^{-1}$ in Table 2 to the frequency law $Q^{-1}(f) = Q_0^{-1}(f) \times f^{-\nu}$ we obtained that $Q_{0i}^{-1} = (11.6 \pm 2.1) \times 10^{-3}$, $\nu_i = 0.7 \pm 0.1$; $Q_{0s}^{-1} = (21.8 \pm 4.7) \times 10^{-2}$, $\nu_s = 1.4 \pm 0.1$; and $Q_{0t}^{-1} = (22.3 \pm 4.5) \times 10^{-2}$, $\nu_t = 1.3 \pm 0.1$.

Table 2 shows that, on average, g values are a factor of 3–10 greater than h estimates, which indicate that scattering is predominant over intrinsic absorption for the studied frequencies.

A comparative plot of the average attenuation parameters Q_i^{-1}, Q_s^{-1}, and Q_t^{-1} as a function of frequency (Table 2) is shown in Fig. 5. It is observed that scattering strongly prevails over intrinsic absorption for all frequencies, indicating that total attenuation is mainly

Table 2
Average S-wave attenuation parameters for the analyzed frequency bands in the Galeras volcanic complex region. $\bar{g} = (1/n)\sum_{j=1}^{n} g_j$; $\bar{h} = (1/n)\sum_{j=1}^{n} h_j$; $\bar{l} = (1/n)\sum_{j=1}^{n} 1/g_j$; and $\bar{l}_a = (1/n)\sum_{j=1}^{n} 1/h_j$, where n is the sample size. The error intervals represent the 95% confidence intervals ($1.96\sigma/\sqrt{n}$).

Center frequency, Hz	$\bar{g}$, km^{-1}	$\bar{h}$, km^{-1}	$\bar{l}$, km	$\bar{l}_a$, km	$\bar{Q}_i^{-1} \times 10^3$	$\bar{Q}_s^{-1} \times 10^2$	$\bar{Q}_t^{-1} \times 10^2$
1.5	0.453 ± 0.043	0.033 ± 0.006	2.7 ± 1.4	77.1 ± 19.0	7.9 ± 1.4	10.7 ± 1.0	11.5 ± 1.2
3.0	0.448 ± 0.024	0.048 ± 0.002	2.8 ± 0.2	36.1 ± 4.9	5.6 ± 0.4	5.3 ± 0.2	5.9 ± 0.2
6.0	0.329 ± 0.039	0.063 ± 0.004	4.4 ± 0.4	20.9 ± 2.4	3.7 ± 0.2	1.9 ± 0.2	2.3 ± 0.2
10.0	0.191 ± 0.043	0.053 ± 0.008	8.1 ± 1.4	24.8 ± 5.1	1.9 ± 0.2	0.7 ± 0.2	0.9 ± 0.2

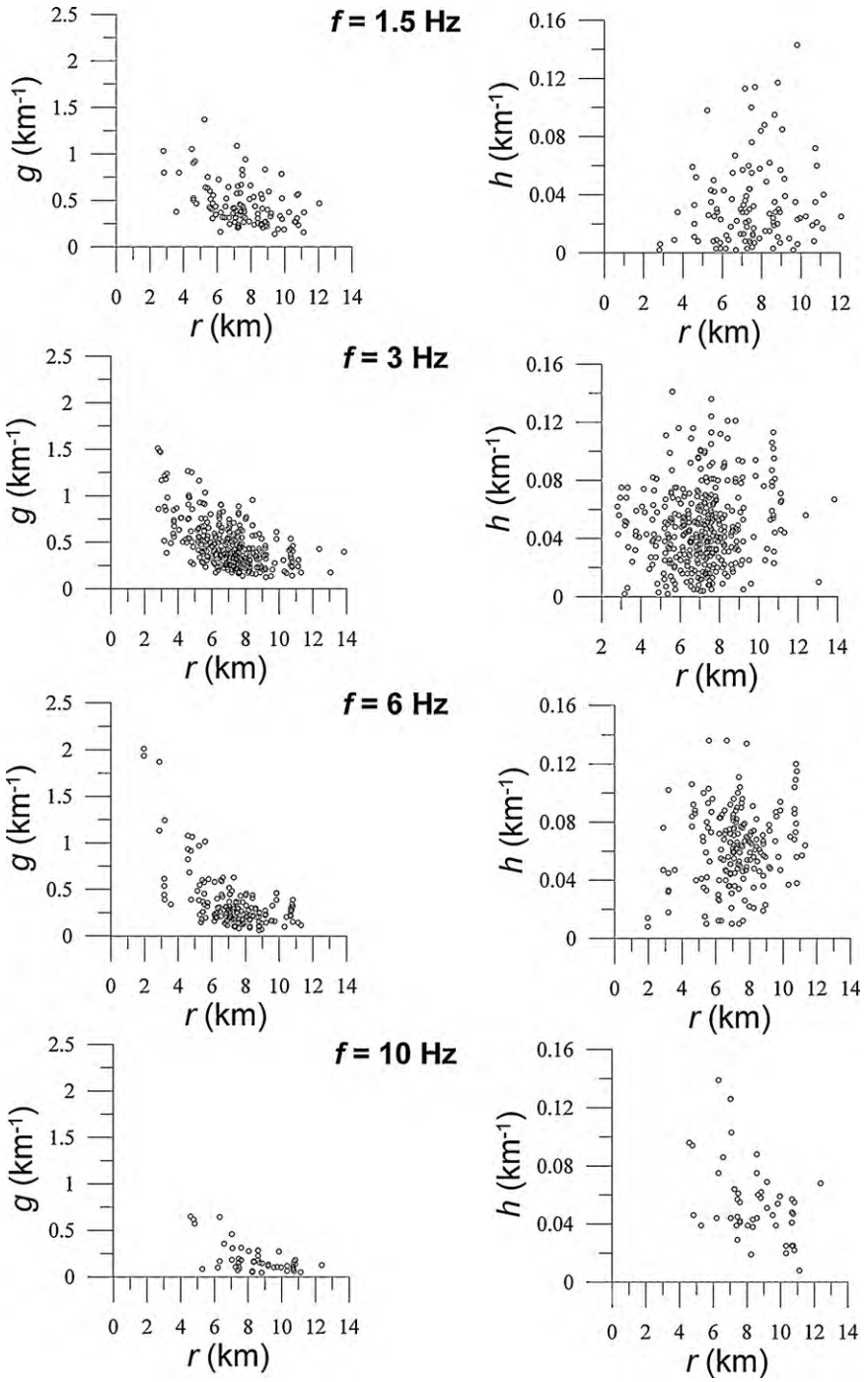

Fig. 6. Plots of *g* (left) and *h* (right) as function of hypocentral distance for the four studied frequency bands.

determined by the scattering loss in the Galeras volcanic complex region.

Finally, Fig. 6 shows the dependence of g and h estimations on the hypocentral distance in the Galeras volcano region. The envelope-fitting method does not require to consider homogeneity for the maximum travel distance range, as in the MLTWA. Thus, a distance dependence of the attenuation parameters can be observed. In Fig. 6 *g* appears to decrease as hypocentral distance increases for all the frequency bands analyzed. According to the events and stations distribution in the target region (see Fig. 1), larger hypocentral distances correspond to larger depths of the hypocenter. Thus, this result may suggest a decrease of heterogeneity with depth in the Galeras volcano region. As for the intrinsic absorption coefficient, no clear trend is observed in Fig. 6.

5.2. Comparison with other volcanic regions

The predominance of scattering over intrinsic dissipation has been found in other volcanoes. Wegler and Lühr (2001) studied the seismic structure of the Merapi volcano (Java) using recordings of artificial shots. They adopted the diffusion model for coda envelope analysis and found that the scattering attenuation is at least one order of magnitude larger than intrinsic absorption. They obtained an extremely short mean free path of the order of $l \simeq 0.1$ km for the frequency range 4–20 Hz. Wegler (2003, 2004) obtained similar

results for Mt. Vesuvius. He again modeled coda envelopes from an active seismic experiment using the diffusion model and found a mean free path for S waves of $l \simeq 0.2$ km for center frequencies between 2 and 16 Hz.

Del Pezzo et al. (2006) obtained different results for Mt. Vesuvius (see also Ugalde and Carcolé, 2009; Del Pezzo et al., 2009). These authors, using volcano-tectonic earthquakes, estimated values of the mean free path for scattering of $l \simeq 0.7$ km for frequencies centered at 3 and 6 Hz and $l > 5$ km for frequencies greater than 6 Hz for one station, and $l \simeq 0.5$ km for the whole frequency range at a second station. They concluded that the diffusion regime was appropriate to model the coda envelopes at Vesuvius volcano.

Very recently Yamamoto and Sato (2010) studied the shallow part of Asama volcano on the basis of the radiative transfer theory using the multiple isotropic scattering model including mode conversions. Using data from an active seismic experiment they obtained a mean free path for scattering of about 1 km for the frequency band 8–16 Hz.

In the present work, we have obtained values of $2.7 \leq l \leq 8.1$ km for frequencies ranging from 1 to 12 Hz. These values are higher than the ones obtained in the Vesuvius, Merapi and Asama vicinities, but they are still much lower than the usual regional measurements reported throughout the world (e.g., Sato and Fehler, 1998, Figure 3.10). Our estimates for the mean free path for scattering are also lower than those obtained by Lemzikov (2008) for the Klyuchevskoi volcanic edifice. By means of a MLTWA applied to volcano-tectonic earthquakes, they obtained values of $8.9 \leq l \leq 34.0$ km at different stations and for frequencies ranging from 0.75 to 18 Hz, which were also consistent with those obtained for Mount Etna (Del Pezzo et al., 1996). The characteristic length scale of intrinsic absorption in the Galeras volcanic complex region gives values of $25 \leq l_a \leq 77$ km. These values are of the same order of magnitude as the usual average findings for other regions (e.g., Sato and Fehler, 1998, Figure 7.12; Lemzikov, 2008), however, the typical length scale for the intrinsic attenuation in this work is at least one order of magnitude larger than the estimates by Wegler (2003) and Wegler and Lühr (2001) at the Vesuvius and Merapi volcanoes, respectively.

In view of the different methods used in the different studies, it is worth examining the assumptions inherent in ours. Therefore, one has to be extremely careful when getting conclusions.

5.3. Influence of the assumptions of the physical model considered

The assumptions underlying the physical model used in this study are similar to those that many researchers used in other regions of the world. The theoretical model used assumes spherically symmetric radiation from the source, although radiated energy is always nonspherical (Sato and Fehler, 1998). The nonspherical radiation from the earthquake source causes a variation in amplitude near the direct S-arrival. Fig. 4 shows scatter among the individual g and h estimates for each frequency band that may be due to fluctuations in the absorption and scattering properties of the crust, but also possibly biased by the anisotropy of the source radiation pattern.

However, the anisotropy of scattering and the vertical heterogeneity of the medium are the most important factors that can bias our estimates from reality. Scattering patterns are nonisotropic in general, and forward scattering strength increases with increasing frequency. Sato and Fehler (1998, p. 214) showed that strong forward scattering increases the amplitude just after the direct-wave arrival, and weak backward scattering decreases the amplitude of the late S-coda as compared to the isotropic scattering case. Abubakirov (2005) noted that the scattering coefficient g obtained within the framework of the multiple isotropic scattering model corresponds roughly to $g_e/2$, where g_e is the effective scattering coefficient. This effective scattering coefficient is related to the true anisotropic scattering coefficient g_s by the equation $g_e = g_s \langle \cos\theta \rangle$, where $\langle \cos\theta \rangle$ is the average cosine of the scattering angle. This implies an important but unknown error in the computation of the mean free paths.

Another factor the model does not take into account is the radiative loss into a weakly scattering mantle (Margerin et al., 1998, 1999). Using the diffusion approximation, Wegler (2004) derived interesting analytical expressions for the coda decay including the leakage of energy from a heterogeneous layer over a homogeneous half-space. He applied the model to seismic data from an active seismic experiment at Vesuvius volcano and he found that there was a trade-off between the intrinsic attenuation and the thickness of the scattering layer. Therefore, a bias to the estimate of h can be introduced by assuming a simple statistically homogeneous half-space model.

Nevertheless, analytical solutions of the radiative transfer equation for a medium with such effects incorporated simultaneously (nonspherical radiation pattern of the source, anisotropy of scattering and inhomogeneity of the scattering and absorption properties) have not yet been found. The approximate method that we use is convenient and could be improved, but is not discrepant with results from previously-used methodologies.

6. Conclusions

Using a coda-envelope-fitting-method, the scattering and intrinsic absorption strengths (g and h) have been estimated for the Galeras volcanic complex region of south western Colombia. The synthetics are calculated by means of the approximate solution of the radiative transfer equation in 3-D given by Paasschens (1997). The method gives a single estimate of the attenuation parameters for each hypocenter-station path and it does not require choosing an arbitrary reference time in order to normalize the waveforms. The method appears to be particularly useful when the dataset characteristics, as in the case of the Galeras volcanic complex, do not allow applying the MLTWA. However, it seems that the envelope-fitting method could be used to analyze any other region.

Results show that the scattering mechanism predominates in the attenuation process in the region for the whole frequency band analyzed. The numerical values obtained in this work for the scattering mean free path ($2.7 \leq l \leq 8.1$ km) are about two orders of magnitude smaller than average estimates for the Earth's crust, which are on the order of $l \approx 100$ km. The characteristic length scale of intrinsic absorption gives values of $25 \leq l_a \leq 77$ km, which are of the same order as the usual values for the Earth's crust. The scattering coefficient seems to decrease with depth whereas the intrinsic absorption parameter does not show any clear trend with distance from the source. We have compared our results with other volcanic regions, and find some discrepancies that might be methodological. The estimates of intrinsic absorption and scattering presented in this study are obtained on the framework of a model based on multiple isotropic scattering, impulsive isotropic point source, and a medium with homogeneous scattering and absorption properties. However, anisotropy of scattering and the vertical heterogeneity of the medium are major factors that may produce biased estimates from the true scattering and absorption coefficients. Therefore, further efforts should be addressed to consider theoretical models with both effects incorporated simultaneously.

Acknowledgments

We are very grateful to the people of the *Observatorio Vulcanológico y Sismológico de Pasto*, Colombia, for providing us with the seismic data used in this study. We thank the Editor, George

Helffrich, and two anonymous reviewers for suggestions that significantly improved the manuscript. This work started when one of the authors (E. C.) was under a "*Juan de la Cierva*" contract of the Spanish *Ministerio de Ciencia y Tecnologia* (*MCYT*). E.C. is now enjoying a fellowship of Global Center of Excellence program for Earth Science in Tohoku University, Sendai, Japan. This research has been partially supported by the MCYT projects CGL-2005-04541-C03-02/BTE and CGL2008-00869/BTE.

References

Abubakirov, I.R., 2005. Attenuation characteristics of transverse waves in the lithosphere of Kamchatka estimated from observations at the Petropavlovsk digital broadband station, Izvestiya. Phys. Solid Earth 41, 813–824.

Banks, N.G., Calvache, M.L., Williams, S.N., 1997. ^{14}C ages and activity for the past 50 ka at Volcán Galeras, Colombia. J. Volcanol. Geotherm. Res. 77, 39–55.

Calvache, M.L., Cortés, G.P., Williams, S.N., 1997. Stratigraphy and chronology of the Galeras volcanic complex, Colombia. J. Volcanol. Geotherm. Res. 77, 5–19.

Carcolé, E., Ugalde, A., Vargas, C.A., 2006. Three-dimensional spatial distribution of scatterers in Galeras volcano, Colombia. Geophys. Res. Lett. 33, L08307, doi:10.1029/2006GL025751.

Carcolé, E., Sato, H., 2010. Spatial distribution of scattering loss and intrinsic absorption of short-period S waves in the lithosphere of Japan on the basis of the Multiple Lapse Time Window Analysis of Hi-net data. Geophys. J. Int. 180, 268–290.

Del Pezzo, E., Simani, M., Ibáñez, J.M., 1996. Separation of intrinsic *Q* for volcanic areas: a comparison between Etna and Campi Flegrei. J. Volcanol. Geotherm. Res. 70, 213–219.

Del Pezzo, E., Bianco, F., Zaccarelli, L., 2006. Separation of Q_i and Q_s from passive data at Mt. Vesuvius: a reappraisal of the seismic attenuation estimates. Phys. Earth Planet. Int. 159, 202–212.

Del Pezzo, E., Bianco, F., Zaccarelli, L., 2009. Reply to comments on "Separation of Q_i and Q_s from passive data at Mt. Vesuvius: A reappraisal of the seismic attenuation estimates" by Ugalde, A. and Carcolé, E. Phys. Earth Planet. Int. 173, 195–196, doi:10.1016/j.pepi.2008.10.002.

Fehler, M., Hoshiba, M., Sato, H., Obara, K., 1992. Separation of scattering and intrinsic attenuation for the Kanto-Tokai region, Japan, using measurements of S-wave energy vs. hypocentral distance. Geophys. J. Int. 108, 787–800.

Gómez, D.M., Torres, R.A., 1997. Unusual low-frequency volcanic seismic events with slowly decaying coda waves observed at Galeras and other volcanoes. J. Volcanol. Geotherm. Res. 77, 173–193.

Hoshiba, M., 1991. Simulation of multiple scattered coda wave excitation based on the energy conservation law. Phys. Earth Planet. Int. 67, 123–136.

Hoshiba, M., 1993. Separation of scattering attenuation and intrinsic absorption in Japan using the Multiple Lapse Time Window Analysis of full seismogram envelope. J. Geophys. Res. 98 (15), 809–815, 824.

Hoshiba, M., Sato, H., Fehler, M., 1991. Numerical basis of the separation of scattering and intrinsic absorption from full seismogram envelope: a Monte-Carlo simulation of multiple isotropic scattering. Pap. Meteorol. Geophys. 42, 65–91.

Hoshiba, M., Rietbrock, A., Scherbaum, F., Nakahara, H., Haberland, C., 2001. Scattering attenuation and intrinsic absorption using uniform and depth dependent model—application to full seismogram envelope recorded in Northern Chile. J. Seismol. 5, 157–179.

Ishimaru, A., 1978. Wave Propagation and Scattering in Random Media. Academic Press, New York.

Lemzikov, M.V., 2008. Estimation of shear-wave attenuation characteristics for the Klyuchevskoi volcanic edifice. J. Volcanol. Seismol. 2, 108–117.

Matsunami, K., Nakamura, M., 2004. Seismic attenuation in a nonvolcanic swarm region beneath Wakayama, southwest Japan. J. Geophys. Res. 109, B09302, doi:10.1029/2003JB002758.

Margerin, L., Campillo, M., Van Tiggelen, B.A., 1998. Radiative transfer and diffusion of waves in a layered medium: new insight into coda Q. Geophys. J. Int. 134, 596–612.

Margerin, L., Campillo, M., Shapiro, N.M., Van Tiggelen, B.A., 1999. Residence time of diffuse waves in the crust as a physical interpretation of coda Q: application to seismograms recorded in Mexico. Geophys. J. Int. 138, 343–352.

Moncayo, E., Vargas, C.A., Durán, J., 2004. Temporal variation of coda-Q at Galeras volcano, Colombia. Earth Sci. Res. J. 8, 19–24.

Paasschens, J.C.J., 1997. Solution of the time-dependent Boltzmann equation. Phys. Rev. E 56, 1135–1141.

Sato, H., 1993. Energy transportation in one- and two-dimensional scattering media: analytic solutions of the multiple isotropic scattering model. Geophys. J. Int. 112, 141–146.

Sato, H., Fehler, M.C., 1998. Seismic wave propagation and scattering in the heterogeneous earth. In: AIP Series in Modern Acoustics and Signal Processing. Springer-Verlag, New York.

Sens-Schönfelder, C., Wegler, U., 2006. Radiative transfer theory for estimation of the seismic moment. Geophys. J. Int. 167, 1363–1372.

Ugalde, A., Tripathi, J.N., Hoshiba, M., Rastogi, B.K., 2007. Intrinsic and scattering attenuation in western India from aftershocks of the 26 January, 2001 Kachchh earthquake. Tectonophysics 429, 111–123.

Ugalde, A., Carcolé, E., 2009. Comments on "Separation of Q_i and Q_s from passive data at Mt. Vesuvius: A reappraisal of the seismic attenuation estimates" by E. Del Pezzo, F. Bianco, and L. Zaccarelli, 2006. Phys. Earth Planet. Int. 173, 191–194, doi:10.1016/j.pepi.2008.10.001.

Wegler, U., 2003. Analysis of multiple scattering at Vesuvius volcano, Italy, using data of the TomoVes active seismic experiment. J. Volcanol. Geotherm. Res. 128, 45–63.

Wegler, U., 2004. Diffusion of seismic waves in a thick layer: theory and application to Vesuvius volcano. J. Geophys. Res. 109 (B7), doi:10.1029/2004JB003048.

Wegler, U., Lühr, B.-G., 2001. Scattering behaviour at Merapi volcano (Java) reveled from an active seismic experiment. Geophys. J. Int. 145, 579–592.

Williams, S.N., Calvache, M.L., Sturchio, N.C., Zapata, J.A., Méndez, R.A., Calvache, B., Londoño, A., Gil, F., Sano, Y., 1990. Premonitory geochemical evidence of magmatic reactivation of Galeras volcano, Colombia. EOS 71 (17), 647.

Yamamoto, M., Sato, H., 2010. Multiple scattering and mode conversion revealed by an active seismic experiment at Asama volcano, Japan. J. Geophys. Res., doi:10.1029/2009JB007109.

Zeng, Y., 1991. Compact solutions for multiple scattered wave energy in time domain. Bull. Seism. Soc. Am. 81, 1022–1029.

Zeng, Y., Su, F., Aki, K., 1991. Scattered wave energy propagation in a random isotropic scattering medium. I. Theory. J. Geophys. Res. 96, 607–619.